

# Antiretrovirally Active Drug Hypericin Binds the IIA Subdomain of Human Serum Albumin: Resonance Raman and Surface-Enhanced Raman Spectroscopy Study

Pavol Miškovský,<sup>\*,†</sup> Daniel Jancura,<sup>†</sup> Santiago Sánchez-Cortés,<sup>‡</sup> Eva Kočíšová,<sup>†</sup> and Laurent Chinsky<sup>§</sup>

Contribution from the Department of Biophysics, P. J. Šafárik University, Jesenná 5, 041 54 Košice, Slovakia, Instituto de Estructura de la Materia, CSIC, Serrano, 121, 28006 Madrid, Spain, and LPBC (CNRS URA 2056), Université P. et M. Curie, Case 138, 4 Place Jussieu, 75231 Paris Cedex 05, France

Received December 15, 1997

**Abstract:** Resonance Raman and surface-enhanced Raman spectroscopy were employed to study the interaction of hypericin with human serum albumin. The identification of the binding place for hypericin as well as the model for albumin–hypericin complex are presented. In this model hypericin interacts with tryptophan placed in II A subdomain of albumin. This interaction reflects (i) a change of the hydrophobicity of the tryptophan environment, (ii) the formation of an H-bond between the carbonyl group of hypericin and N1–H group of tryptophan, leading to a protonated-like carbonyl in the drug, (iii) a decrease of the strength of H bonding at the N1–H site of tryptophan, and (iv) a change of the tryptophan side-chain conformation.

## Introduction

Hypericin (Figure 1) is a natural photosensitizing polycyclic aromatic dione that can be extracted from plants of the *Hypericum* genus.<sup>1</sup> It displays virucidal activity against several types of viruses, including the human immunodeficiency virus (HIV),<sup>2–4</sup> as well as antiproliferative and cytotoxic effects on tumor cells.<sup>5–7</sup> Its virucidal activity is enhanced more than 100-fold in the presence of light.<sup>4,8</sup> Other different biological properties of hypericin have been described, such as potent antidepressive activity,<sup>9</sup> light-dependent inhibition of protein kinase C,<sup>5,10</sup> tyrosine kinase activity,<sup>11</sup> and photosensitized inhibition of mitochondrial succinoxidase.<sup>12</sup> Hypericin, like many other anticancer drugs, has also been reported to induce

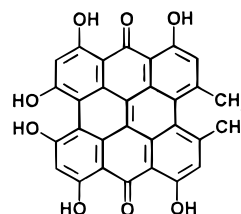


Figure 1. Hypericin structure.

apoptosis.<sup>7</sup> Biological activity of hypericin and related compounds has been reviewed by Diwu et al.<sup>13</sup>

Serum albumin as the most abundant plasma protein contributes significantly to many transport and regulatory processes. The protein binds a wide variety of substrates such as metals, fatty acids, amino acids, hormones, and an impressive spectrum of therapeutic drugs.<sup>14</sup> Because of its clinical and pharmaceutical importance, interaction of serum albumin with a variety of ligands has been studied extensively.<sup>15–19</sup>

The hypericin–human serum albumin (HSA) complex was studied by various groups.<sup>20–22</sup> The binding properties of hypericin to HSA help to overcome difficulties in solubilization and dispersion of hypericin in aqueous physiological solution. The HSA–hypericin interaction results in dissociation into the monomeric form of hypericin, which is aggregated in the

\* E-mail: misko@kosice.upjs.sk.

† Šafárik University.

‡ CSIC.

§ Université P. et M. Curie.

(1) Duran, N.; Song, P. S. *Photochem. Photobiol.* **1986**, *48*, 667–680.

(2) Meruelo, D.; Lavie, G.; Lavie, D. *Proc. Natl. Acad. Sci. U.S.A.* **1988**, *85*, 5230–5234.

(3) Kraus, G. A.; Pratt, D.; Tøsseberg, J.; Carpenter, S. *Biochem. Biophys. Res. Commun.* **1990**, *172*, 149–153.

(4) Lenard, J.; Rabson, A.; Vanderoef, R. *Proc. Natl. Acad. Sci. U.S.A.* **1993**, *90*, 158–162.

(5) Takahashi, I.; Nakanishi, S.; Kobayashi, E.; Nakano, H.; Suzuki, K.; Tamaoki, T. *Biochem. Biophys. Res. Commun.* **1989**, *165*, 1207–1212.

(6) Andreoni, A.; Colasanti, A.; Colasanti, P.; Mastrocinque, M.; Riccio, P.; Roberti, G. *Photochem. Photobiol.* **1994**, *59*, 529–533.

(7) Couldwell, W. T.; Gopalakrishna, R.; Hinton, D. R.; He, S.; Weiss, M. H.; Law, R. E.; Apuzzo, M. L. *Neurosurgery* **1994**, *35*, 705–710.

(8) Carpenter, S.; Kraus, G. A. *Photochem. Photobiol.* **1991**, *53*, 169–174.

(9) Okpanyi, S. N.; Weischer, M. L. *Arzneimittel-Forschung* **1987**, *37*, 10–13.

(10) Utsumi, T.; Okuma, M.; Utsumi, T.; Kanno, T.; Yasuda, T.; Kobuchi, H.; Horton, A. A.; Utsumi, K. *Arch. Biochem. Biophys.* **1995**, *316*, 493–497.

(11) De Witte, P.; Agostinis, P.; Van Lint, J.; Merlevede, W.; Vandenhede, J. R. *Biochem. Pharmacol.* **1993**, *46*, 1929–1936.

(12) Thomas, C.; MacGill, R. S.; Miller, G. C.; Pardini, R. S. *Photochem. Photobiol.* **1992**, *55*, 47–53.

(13) Diwu, Z. *Photochem. Photobiol.* **1995**, *61*, 529–539.

(14) Peters, T. *Adv. Protein Chem.* **1985**, *37*, 161–245.

(15) Fehske, K. J.; Müller, W. E.; Wollert, U. *Mol. Pharmacol.* **1979**, *16*, 778–789.

(16) Sjöholm, I.; Erman, B.; Kober, A.; Ljungstedt-Pahlman, I.; Seiving, B.; Sjödin, T. *Mol. Pharmacol.* **1979**, *16*, 767–777.

(17) Kragh-Hansen, U. *Mol. Pharmacol.* **1988**, *34*, 160–171.

(18) Davila, J.; Harriman, A. *J. Am. Chem. Soc.* **1990**, *112*, 2686–2690.

(19) Rotenberg, M.; Cohen, S.; Margalit, R. *Photochem. Photobiol.* **1987**, *46*, 689–693.

(20) Lavie, G.; Mazur, Y.; Lavie, D.; Prince, A. M.; Pascual, D.; Liebes, L.; Levin, B.; Meruelo, D. *Transfusion* **1995**, *35*, 392–400.

(21) Senthil, V.; Longworth, J. W.; Ghiron, C. A.; Grossweiner, L. I. *Biochim. Biophys. Acta* **1992**, *115*, 192–200.

(22) Falk, H.; Meyer, J. *Monatsh. Chem.* **1994**, *125*, 753–762.

aqueous phase. The dissociation of hypericin to the monomeric form appears to be crucial for the virucidal action.<sup>20</sup>

The method based on the increase of the hypericin absorption and fluorescence with the increase of albumin concentrations in an aqueous solution was used for the determination of the HSA–hypericin binding constant. The assumption that HSA has a single binding place for hypericin leads to  $K = 7.5 \times 10^5 \text{ M}^{-1}$ .<sup>21</sup> As concerns a binding place of the hypericin in the albumin structure, Falk et al. by means of competition experiments have established that hypericin forms a specific heteroassociation with HSA which involves bonding of hypericin to the III A subdomain of the protein.<sup>22</sup>

The structural changes of albumin and the identification of binding place for hypericin as well as a model for albumin–hypericin interaction are presented in this article. For the study of such a complex system two techniques of Raman spectroscopy have been used: (i) the resonance Raman spectroscopy with an excitation at 222 nm which selectively enhanced the vibrations of the aromatic amino acids of the protein, particularly the tryptophan ones, and (ii) the surface-enhanced Raman scattering technique (SERS) which allowed us to see the hypericin in the complex structure via a strong enhancement of the hypericin vibrations and the quenching of its fluorescence caused by adsorbance of this molecule to the colloidal surface. The high efficiency of the resonance Raman and surface-enhanced Raman spectroscopies for such a type of research has been previously presented in our study of the DNA–hypericin complex.<sup>23</sup>

## Experimental Section

**Chemicals.** HSA used in this study was purchased from Sigma (essentially fatty acid free) and used without further purification. Hypericin was obtained from Carl-Roth. All others reagents employed were of analytical grade and were obtained from Sigma.

**Surface-Enhanced Raman Spectroscopy and Absorption Spectroscopy.** Silver colloids were prepared by following the method of Lee and Meisel.<sup>24</sup> Samples for SERS experiments were prepared by dissolving 1 mg of HSA in 0.2 mL of water. After, 10  $\mu\text{L}$  of a  $7 \times 10^{-4} \text{ M}$  hypericin solution in dimethyl sulfoxide (DMSO) was added, and then the mixture was left for approximately 12 h to allow a complete interaction of the drug with the protein. Samples containing only drug were also aged for the same time at the same conditions. The colloid was activated before being added to the drug–protein complex solution. This activation consisted of a partial aggregation of the colloidal particles, and to accomplish this, 0.15 mL of a 0.5 M sodium nitrate solution was added to 2 mL of the original colloid. Then, 1 mL of this activated colloid was added to the mixture. Samples prepared in such a way were stable for several days. The pH of the final mixture was about 7.0 in all the cases, and the DMSO in the sample was at a concentration of 0.8%.

Raman spectra were recorded by using a JASCO NR-1100 model spectrophotometer. The line at 514.5 nm provided by a Coherent Innova 90 Ar<sup>+</sup> laser model was employed as the excitation. The resolution was set to 2  $\text{cm}^{-1}$ , and a 90° geometry was used to record data. The laser power at the sample was about 20 mW. Spectra shown in this work were recorded at 1  $\text{cm}^{-1}$  step with an integration time of 1 s. All the spectra are presented without any further manipulation.

UV–vis absorption spectra of free hypericin in a water solution (0.8% of DMSO) as well as the UV–vis absorption spectra of HSA–hypericin complex were recorded on a Jasco 7850 spectrophotometer.

**Resonance Raman Spectroscopy.** The solution of HSA for the resonance Raman spectroscopy was prepared in 10 mM, pH 7.2 phosphate buffer at a protein concentration 1 mg/mL. Because of a

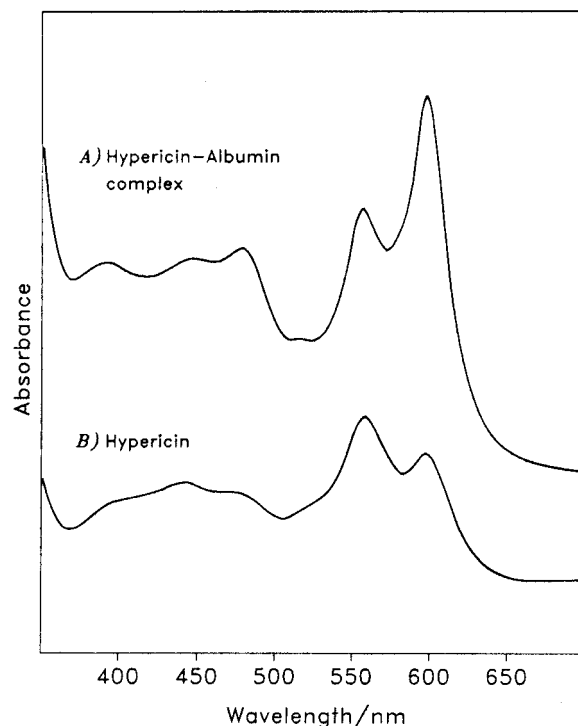


**Figure 2.** Absorption spectra of hypericin ( $3 \times 10^{-6} \text{ M}$ ) in aqueous solution (0.5% in DMSO) in the presence of human serum albumin (A) and in the absence of the protein (B).

strong Raman scattering of DMSO, it was not possible to use a hypericin DMSO solution for the sample preparation. Thus the mixed solution was prepared by adding a pure hypericin to the protein-buffered solution (an excess). These solutions have been gently stirred for 12 h at room temperature to allow a complete interaction of the drug with the albumin.

Resonance Raman spectra of the sample and buffer solutions were obtained in the 400–1800  $\text{cm}^{-1}$  range using a Jobin-Yvon Ramanor HG-2S double monochromator operating in the second order of the gratings and excited by 222 nm excitation line with the average laser power of 1 mW. The 222 nm excitation wavelength was obtained from a Quantel Datachrom 5000 dye laser (Rhodamine 590 perchlorate dye) pumped with a Quantel Nd:YAG pulsed laser and by using various mixing and doubling crystals. The incident illumination of the sample was controlled by a monitoring pathway consisting of the external photomultiplier irradiated with a small fraction of the incident laser beam. The Raman signal was that rationed to the monitoring signal in the data processing device. Spectra presented in this paper are the averages of five consecutive scans recorded at 1  $\text{cm}^{-1}$  steps. To exclude an eventual thermal degradation of the samples caused by light absorption, the samples have been stirred in the sample cell at a temperature of 4 °C. The subtraction of a weak Raman contribution of the buffer as well as the intensity normalization of the spectra, needed before proceeding to spectral differences was made using a strong water O–H stretching band at 3450  $\text{cm}^{-1}$ . The spectra were smoothed using a fast Fourier transform method. To exclude eventual modulations in the spectra caused by the smoothing procedure, the spectra of samples with different preparation were recorded. For all of these spectra a high reproducibility has been obtained even for the low-intensity bands.

## Results and Discussion

**UV–Vis Absorption Spectra of Hypericin–Albumin Complex.** Figure 2 shows the absorption spectra of hypericin and the HSA–hypericin complex in aqueous solution. The spectral profile of hypericin alone is markedly affected by complexation with the protein. The main changes that we can observe in the complex are a remarkable enhancement of the 599 nm band and a considerable profile change in the 400–500 nm region.

(23) (a) Miskovsky, P.; Chinsky, L.; Wheeler, G. V.; Turpin, P. Y. *J. Biomol. Struct. Dyn.* **1995**, *13*, 547–552. (b) Sánchez-Cortés, S.; Miskovsky, P.; Jancura, D.; Bertoluzza, A. *J. Phys. Chem.* **1996**, *100*, 1938–1944.

(24) Lee, P. C.; Meisel, D. *J. Phys. Chem.* **1982**, *86*, 3391–3395.

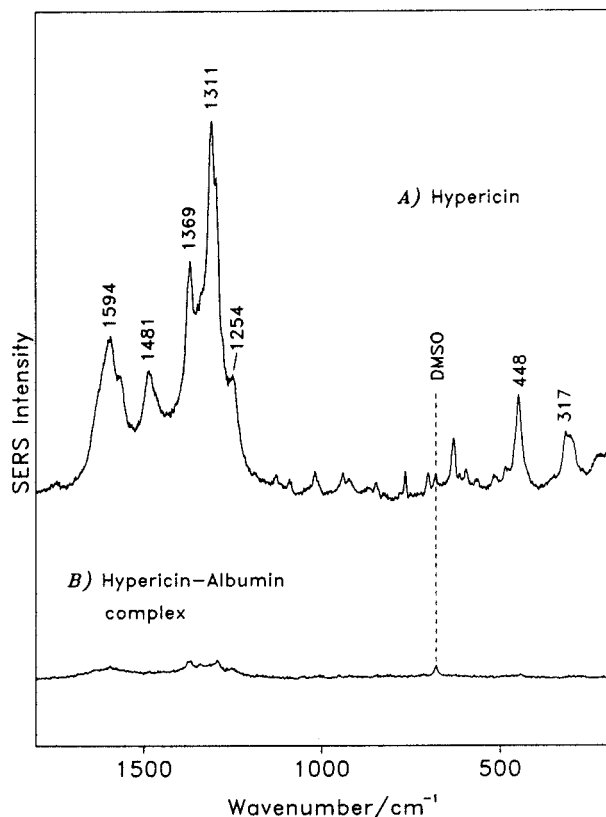


**Figure 3.** SERS spectra of hypericin ( $3 \times 10^{-6}$  M) in silver aqueous colloid in the absence (A) and in the presence (B) of human serum albumin. The  $680 \text{ cm}^{-1}$  DMSO band was taken as a reference.

The complex spectrum is very similar to that of hypericin in a solution of dimethyl sulfoxide (DMSO). This indicates that albumin induces a solubilization of the drug in water due to interaction with the protein as was also proposed by van Senthil *et al.*<sup>21</sup>

**SERS of Hypericin–Albumin Complex.** Figure 3 shows the SERS spectrum of hypericin (Figure 3a) and the hypericin/albumin complex (Figure 3b) normalized on the DMSO Raman band ( $680 \text{ cm}^{-1}$ ). The complex spectrum is dominated by hypericin bands due to selective enhancement of the drug bands at this excitation wavelength. Two main features can be observed in the complex spectrum in relation to that of hypericin: (i) a relative intensity decrease and (ii) a change in the spectral profile. As the normalized complex spectrum is a very low intensity spectrum we present it also not normalized in Figure 4c to discuss the individual bands changes caused by the complex formation.

The intensity decrease is clearly demonstrated in Figure 3 by taking the  $680 \text{ cm}^{-1}$  DMSO band as the internal standard, demonstrating the existence of a strong interaction between the drug and the protein. Since the albumin concentration is 4 times more concentrated than the drug, we suppose that all hypericin molecules interact with the albumin and, consequently, the SERS spectrum of Figure 3b must correspond to the hypericin involved in the complex. Moreover, the weakness of hypericin bands in the complex Raman spectrum can be attributed to steric hindrance caused by interaction with the protein. According to the electromagnetic model of SERS, there exists a high electromagnetic field gradient and, consequently, a great dependence of SERS signal with the distance to the surface. Therefore, the weakness of the complex SERS signal may be due to the long distance at which the drug is placed in relation to the surface. This fact indicates that the hypericin site of

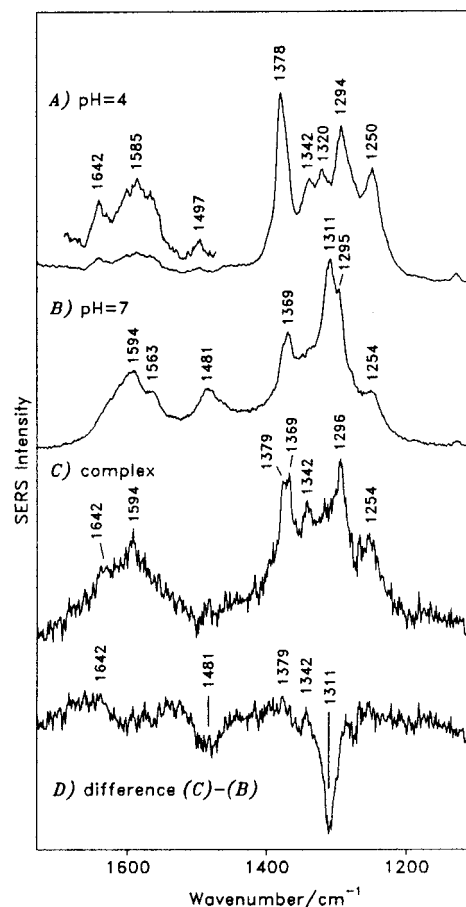


**Figure 4.** SERS spectra of hypericin ( $3 \times 10^{-6}$  M) in the  $1100\text{--}1700 \text{ cm}^{-1}$  region: (A) at pH = 4; (B) pH = 7. (C) SERS spectrum of hypericin–HSA complex and (D) difference spectrum between the SERS of the complex and SERS of hypericin at neutral pH.

binding in albumin may be placed in the inner part of the protein, since its accessibility to the metallic surface is markedly limited when forming part of the complex.

In Figure 4 the spectral profiles of hypericin and complex SERS (surface-enhanced resonance Raman spectroscopy) spectra are shown. For better comparison of the differences between these two spectra we have obtained also the difference spectra (Figure 4d). In the complex spectrum, relative enhancements of bands at  $1254$ ,  $1345$ ,  $1369$ , and  $1642 \text{ cm}^{-1}$  can be seen, with an upshift of the  $1369 \text{ cm}^{-1}$  band toward  $1379 \text{ cm}^{-1}$ , as well as intensity decrease of bands at  $1311$  and  $1481 \text{ cm}^{-1}$ . Similar changes can be observed in the hypericin SERS spectrum at acidic pH (Figure 4a), where an enhancement of the intensity and a profile change are also observed. In fact, at low pH, a protonation of carbonyl group occurs, this leading to a breakdown of intermolecular bonds existing between the drug molecules in aqueous solution. The solubilization of the drug at acidic pH increases the amount of monomeric drug in solution, and consequently, the adsorbed hypericin on the surface of the colloid is also increased. Protonation of carbonyl groups induces a strong decrease of  $1311$  and  $1585 \text{ cm}^{-1}$  bands, and an intensity increase of bands at  $1248$ ,  $1320$ ,  $1342$ ,  $1379$ , and  $1642 \text{ cm}^{-1}$ . The band at  $1642 \text{ cm}^{-1}$  is attributed to carbonyl stretching motions. Its presence in both the complex and protonated hypericin indicates that it is due to monomeric hypericin resulting after disruption of intermolecular bonds of hypericin aggregates. The band at  $1311 \text{ cm}^{-1}$  is pH sensitive, and thus, it can be attributed to ring motions coupled to carbonyl vibrations.<sup>25</sup> This band completely disappears at low pH and

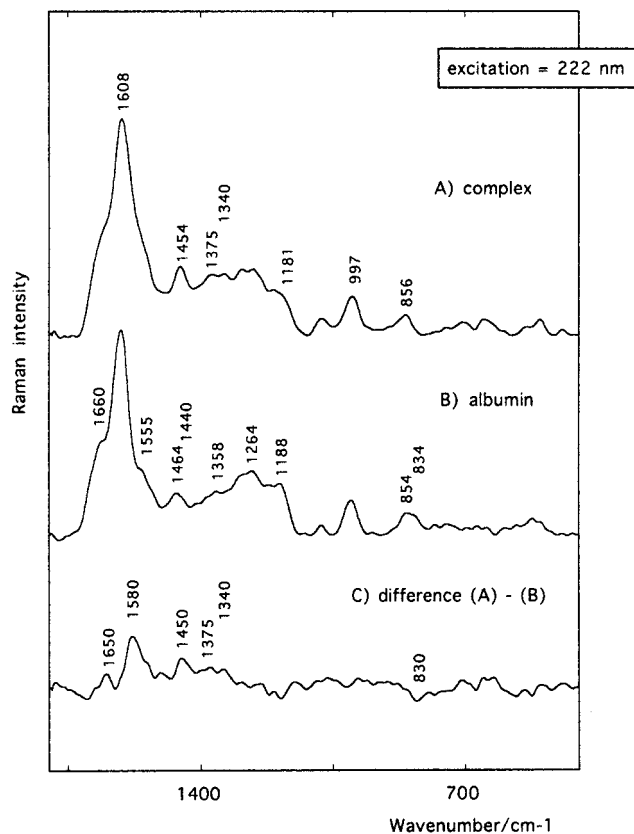


**Figure 5.** Resonance Raman spectra of HSA–hypericin complex (A) and free HSA (B) and the difference spectrum between the complex and free HSA (C).

by complexation with albumin, thus indicating the existence of an albumin interaction through the carbonyl group.

Thus the similarities found between the protonation of hypericin and complexation with albumin suggest that the interaction with the protein implies (i) a disruption of the intermolecular H-bonds existing between the drug molecules,<sup>26,27</sup> with solubilization of hypericin in aqueous solution, and (ii) an establishment of an H-bond between the carbonyl groups of hypericin and a hydrogen donor of albumin, leading to a protonated-like carbonyl in the drug.

**Resonance Raman Spectra of Hypericin–Albumin Complex.** Figure 5 represents the resonance Raman spectra of HSA, the HSA–hypericin complex, and the difference spectrum (complex – HSA) in the region from 400 up to 1800  $\text{cm}^{-1}$  excited with the 222 nm excitation wavelength. This excitation favors the resonance enhancement of the aromatic amino acids,<sup>28–32</sup> the tryptophan vibrations in particular.<sup>28–30</sup>

The main differences in going from HSA to the complex spectrum concern the bands at 854, 1188, 1340, 1464, and 1555  $\text{cm}^{-1}$  (Figure 5). These bands correspond to vibrations of the aromatic amino acids in the human serum albumin structure,

(25) Jancura, D.; Sánchez-Cortés, S.; Kocisova, E.; Tinti, A.; Miskovsky, P.; Bertoluzza, A. *Biospectroscopy* **1995**, *1*, 265–273.

(26) Yamazaki, T.; Ohta, N.; Yamazaki, I.; Song, P. S. *J. Phys. Chem.* **1993**, *97*, 7870–7885.

(27) Sánchez-Cortés, S.; Miskovsky, P.; Jancura, D.; Bertoluzza, A. *Spectrochim. Acta, Part A* **1997**, *53*, 769–779.

(28) Asher, S. A.; Ludwig, M.; Johnson, C. R. *J. Am. Chem. Soc.* **1986**, *108*, 3186–3197.

(29) Rava, R. P.; Spiro, T. G. *J. Am. Chem. Soc.* **1984**, *106*, 4062–4064.

(30) Hirakawa, A. Y.; Nishimura, Y.; Matsumoto, T.; Nakanishi, M.; Tsuboi, M. *J. Raman Spectrosc.* **1978**, *7*, 282–287.

(31) Rava, R. P.; Spiro, T. G. *J. Phys. Chem.* **1985**, *89*, 1856–1861.

(32) Rava, R. P.; Spiro, T. G. *Biochemistry* **1985**, *24*, 1861–1865.

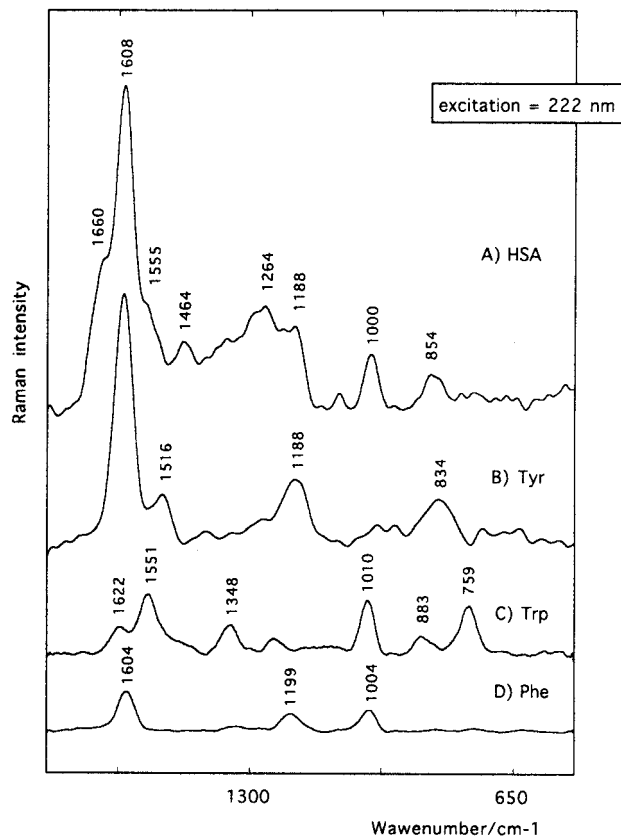


**Figure 6.** Decomposition of the resonance Raman spectra of HSA into the resonance Raman spectra of the aromatic amino acids Trp, Tyr, and Phe.

which contains one tryptophan (Trp), 18 tyrosines (Tyr), and 31 phenylalanines (Phe).<sup>14</sup> Thus, despite the high resonance enhancement for Trp with the 222 nm excitation wavelength in comparison with the Tyr and Phe, our interpretation of the resonance Raman bands of albumin is based on the albumin spectrum decomposition into the resonance Raman spectra of the Trp, Tyr, and Phe obtained for the same excitation wavelength (Figure 6). From this decomposition one can observe that the 222 nm excitation spectrum of albumin is mainly composed of high enhanced Trp bands except the 854 and 1188  $\text{cm}^{-1}$  Tyr mode and the complex band at 1608  $\text{cm}^{-1}$ , which is due to a combination of Trp, Tyr, and Phe. The appearance of the Tyr vibration modes in the HSA spectrum for this excitation wavelength, which favors the resonance enhancement of Trp, is caused by the high amount of Tyr residues in the comparison with one Trp (18 Tyr: 1 Trp). From the point of view of the complex structure interpretation, the observed spectral changes in going from the HSA to the HSA–hypericin complex mainly reflect (i) a decrease of the strength of H bonding at the N1–H site of Trp, (ii) a change of the Trp side-chain conformation, and (iii) a change of the hydrophobicity of the Trp environment.

The doublet of the Trp bands at 1438 and 1460  $\text{cm}^{-1}$  has been found to be sensitive to the N1–H hydrogen bonding.<sup>34</sup> This doublet corresponds to the Trp bands observed at 1434 and 1462  $\text{cm}^{-1}$  excited by 218 nm excitation wavelength,<sup>30</sup> which are enhanced in the albumin spectrum in comparison to the tryptophan alone, as a consequence of HSA structure formation. These lines were assigned to the in plane skeletal

(33) Miura, T.; Takeuchi, H.; Harada, I. *Biochemistry* **1988**, *27*, 88–94.

(34) Maruyama, T.; Takeuchi, H. *J. Raman Spectrosc.* **1995**, *26*, 319–324.

modes of pyrrole ring<sup>30,35</sup> with a large contribution of the N1–H bend in particular for the 1438 cm<sup>-1</sup> line.<sup>36</sup> These vibrations were found to be very sensitive to N1–H environment of the Trp and proposed as markers of hydrogen bonding. Their frequencies increase with an increase of the hydrogen bonding strength.<sup>33</sup> In our spectra the downshift and the intensity increase of the large band at 1464 cm<sup>-1</sup> with a shoulder at 1440 cm<sup>-1</sup> was observed as a consequence of the HSA–hypericin complex formation (Figure 5). Thus the behavior of this doublet in the albumin spectra (Figure 5) indicates a decrease of the strength of H bonding at the N1–H site of tryptophan caused by the HSA–hypericin complex formation. Taking into account our results obtained by SERS spectroscopy where a protonation of the carbonyl group of hypericin was observed as a consequence of an interaction with a proton donor in the albumin structure, we propose that the decrease of the H bonding strength is caused by an hydrogen bond formation between the N1–H position of Trp and the carbonyl group of hypericin.

The observed interaction of the hypericin molecule with Trp via hydrogen bond formation provokes a conformation change of the Trp side chain. An upshift of a 1555 cm<sup>-1</sup> shoulder in HSA (Figure 5b) is observed upon the complex formation. A strong positive band at 1580 cm<sup>-1</sup> in the difference spectrum reflects this shift (Figure 5c). It was shown by Miura *et al.* that this Trp vibration of the N1–C2H–C3–C<sub>β</sub> linkage varies as a function of torsion angle about the C<sub>α</sub>–C<sub>β</sub>–C3–C2 linkage.<sup>36</sup> Thus the HSA–hypericin complex formation leads to the important change (upshift at about 25 cm<sup>-1</sup>) of the torsion angle of the Trp side chain.

With the Trp side-chain deformation a protein conformation change is associated. The structural sensitive Amid I at about 1660 cm<sup>-1</sup> (shoulder) and amid III at 1264 cm<sup>-1</sup> can be observed at HSA spectrum (Figure 5b). The positions of these bands indicate a large  $\alpha$ -helical structure content in the HSA structure.<sup>40</sup> The complex formation induces a downshift of the shoulder at 1660 cm<sup>-1</sup> with the corresponding band at 1650 cm<sup>-1</sup> in the difference spectrum (Figure 5c), while the intensity and the position of the amid III band does not change (Figure 5). These spectral features indicate a partial conformation change of HSA which changes from the  $\alpha$ -helix toward an irregular  $\alpha$ -helix (downshift of amid I band).<sup>40</sup>

From the point of view of the HSA–hypericin complex formation a 1358/1340 cm<sup>-1</sup> (Figure 5b) Fermi doublet behavior is interesting.<sup>37</sup> The intensity ratio of 1360/1340 cm<sup>-1</sup> bands has been found to be a very sensitive indicator of hydrophobicity of the Trp environment.<sup>33</sup> The decrease of this ratio leads to a hydrophobicity increase of the Trp environment.<sup>33</sup> In Figure 5 we can observe an intensity increase of the 1340 cm<sup>-1</sup> doublet component upon the complex formation which can indicate an increase of the hydrophobicity of the Trp environment. The behavior of the 1360 cm<sup>-1</sup> doublet component is more difficult to evaluate because it is partially overlapped by the band at 1375 cm<sup>-1</sup>. The intensity increase of this band can be attributed to the direct interaction of hypericin with N1–H position of Trp since a similar change was observed in the study of the

hydrogen–deuterium exchange of the N1 position of Trp by resonance Raman spectroscopy.<sup>33</sup> Nevertheless, in the difference spectrum (Figure 5c), we can see the positive band at 1340 cm<sup>-1</sup> and a negative one at approximately 1358 cm<sup>-1</sup>, which indicate that the 1360/1340 cm<sup>-1</sup> ratio decreases, and so the hydrophobicity of Trp environment increases upon the HSA–hypericin complex formation.

Thus, the hydrophobic interaction of hypericin with albumin leads to the favorable position of hypericin for the H-binding of its carbonyl group with the N1–H position of Trp which is placed in the IIA subdomain of the protein. As a consequence of this hydrophobic interaction, the hydrogen bond of the Trp–hypericin complex is weaker than the hydrogen bond of N1–H Trp group in the free HSA structure.

From the decomposition of the albumin resonance Raman spectra, one can see that for the 222 nm excitation the tryptophan and tyrosine dominate in the albumin spectrum in comparison to the phenylalanine (Figure 6). This is a consequence of the high resonance enhancement of the Trp vibrations (only one Trp is presented in HSA structure) on the one side and the presence of 18 Tyr residues, which are not so enhanced as Trp, in the HSA structure on the other side. The complex formation leads to the intensity decrease of the 834 cm<sup>-1</sup> Tyr shoulder attributed to the low-frequency component of 853/831 cm<sup>-1</sup> Fermi doublet (Fermi resonance between the symmetric ring breathing and nonplanar ring vibrations).<sup>39</sup> The observed behavior of this doublet upon the complex formation reflects changes of the state of the hydroxyl group of the Tyr residues. Another tyrosine vibration is changed as a consequence of the complex formation. A relative intensity decrease and a downshift of the 1188 cm<sup>-1</sup> Tyr band attributed to the ring vibration of Tyr,<sup>30</sup> to the final position at 1181 cm<sup>-1</sup>, is seen in the resonance Raman spectra (Figure 5). Thus, we have to decide if these changes of the Tyr vibrations are caused by a direct interaction of hypericin with tyrosine or if they are only a consequence of the HSA structural change. The HSA structure contains only one Trp molecule in the IIA subdomain. Using 222 nm excitation wavelength, we can see very clearly that the Trp molecule is in a direct interaction with hypericin (Figure 5), and so, it binds the IIA subdomain of the HSA. The assumption that HSA has a single binding site for hypericin<sup>21</sup> and an excitation wavelength which favors the Trp vibration enhancement makes impossible to identify any spectral change for an individual Tyr molecule which should be eventually in an interaction with hypericin. Thus the observed spectral changes attributed to the Tyr molecules in our resonance Raman spectra of the HSA–hypericin complex (Figure 5) must be associated with a global conformation change of the protein, leading to modification of the environment of about all Tyr and consequently to modification of the discussed Tyr resonance Raman bands.

It is also known that the binding activity of the subdomain IIA affects conformational changes as well as binding affinities in domain IIIA because the binding subdomains share a common interface.<sup>38</sup> Thus from this analysis we can conclude that the observed changes of the Tyr vibrations are caused by the structural changes of the IIA–IIIA interface of the HSA.

## Conclusions

Precise knowledge about location and structure of binding sites on HSA and the binding affinity of different ligands and drugs to these binding sites are useful for understanding and prediction of the ligand–drug displacement interaction and should provide a basis for modifications of the drug to carry

(35) Suwaiyan, A.; Zwarich, R. *Spectrochim. Acta, Part A* **1986**, *42*, 1017–1020.

(36) Miura, T.; Takeuchi, H.; Harada, I. *J. Raman Spectrosc.* **1989**, *20*, 667–671.

(37) Harada, I.; Miura, T.; Takeuchi, H. *Spectrochim. Acta* **1986**, *42*, 307–312.

(38) He, X. M.; Carter, D. C. *Nature* **1992**, *358*, 209–215.

(39) Siamwiza M. N.; Lord, R. C.; Chen, M. C. *Biochemistry* **1975**, *14*, 4870–4876.

(40) Harada, I.; Takeuchi, H. *Spectroscopy of biological systems*; Clark, R. J. H., Hester, R. E., Eds.; John Wiley & Sons Ltd: New York, 1986; pp 113–175.

therapeutic and diagnostic agents. The principal binding regions on HSA are located in hydrophobic cavities in subdomains II A and III A of the protein. The binding cavity in III A is the most active on HSA, and many ligands were found to bind preferentially there (digitoxin, ibuprofen, AZT). Aspirin shows nearly equally distribution between binding sites located in II A and III A domains. Warfarin is known to occupy a single site in II A.<sup>38</sup> Trp 214, conserved in mammalian albumin, plays an important structural role in the formation of the II A binding site by limiting the solvent accessibility, and it participates in an additional hydrophobic packing interaction between II A and III A interface. Changes in absorption, fluorescence, and vibrational spectra of lonely Trp molecule in HSA are often used for the study of ligand–HSA interactions in II A subdomain of the protein.<sup>15,17</sup>

Our SERS spectra of the hypericin and the HSA–hypericin complex indicate a strong interaction between the complex components. This interaction is presented by a strong intensity decrease of the hypericin SERS spectrum when interacting with the albumin (Figure 3). According to the electromagnetic model of SERS, this intensity decrease may be due to the long distance at which the drug is placed in relation to the colloid surface. This fact indicates that hypericin is placed in the inner part of the complex as a consequence of the HSA–hypericin complex formation. Moreover, the detailed study of the hypericin SERS spectra profile and its comparison with the protonated hypericin (Figure 3) indicate the interaction of the carbonyl group of hypericin with a hydrogen donor of albumin, leading to a protonated-like carbonyl in the drug.

The resonance Raman study of the complex indicates that such type of interaction mainly leads to (Figure 5) (i) the change of the hydrophobicity of the environment of Trp, which reflects the intensity increase of the  $1340\text{ cm}^{-1}$  Trp band, (ii) the decrease of the strength of H bonding at the N1–H site of Trp, which reflects the downshift of the  $1464\text{ cm}^{-1}$  Trp band, and (iii) the change of the Trp side-chain conformation, which reflects the upshift of the  $1555\text{ cm}^{-1}$  Trp band.

From these results we can conclude that the hydrophobic interaction of hypericin with HSA leads to the formation of

hydrogen bond between the carbonyl group of hypericin and the N1–H position of Trp located in the IIA subdomain of the HSA structure. Thus our interpretation is not in a direct agreement with the result found by Falk et al.,<sup>22</sup> who have found that hypericin binds the IIIA subdomain of albumin. In fact in our resonance Raman study we have observed some spectral changes associated with Tyr molecule (Tyr 411 is very important for the IIIA binding affinity<sup>38</sup>), but these changes are attributed to global conformational changes of the Tyr molecules as a consequence of the Trp–hypericin interaction.

The HSA structure contains only one Trp molecule located in the IIA subdomain of the HSA. With 222 nm excitation which enhanced Trp vibrations we can see clearly that the hypericin interacts with N1–H position of Trp and so it is located in the IIA subdomain of HSA. This interaction provokes a change of the side-chain conformation of Trp, change of the hydrophobicity of the Trp environment, and influence of global conformation of the HSA molecule. These changes influence the selected vibrations of tyrosine molecules. The disagreement with the results obtained by Falk et al. could be explained by the fact that the binding activity of the subdomain IIA affects conformational changes as well as binding affinities in domain IIIA because the binding subdomains share a common interface.<sup>38</sup>

Thus we can conclude that the hydrophobic interaction of hypericin with IIA subdomain of HSA leads to the formation of the H-binding of carbonyl group of hypericin with the N1–H position of Trp and can create structural changes of the IIA–IIIA interface of HSA.

**Acknowledgment.** This work has been supported by a grant of the Slovak Ministry of Education (No. 1/3258/96) and the fellowships of the Spanish Ministerio de Asuntos Exteriores (Dirección General de Relaciones Culturales y Científicas) (D.J.) and Spanish Ministerio de Education y Ciencia (DGICYT) under the Project PB-93 0973C02-02 (S.S.-C.).

JA974233A